

# Polarity and orbital driven reduction in contact resistance in organic devices with functionalized electrodes

Cite as: J. Chem. Phys. 159, 121102 (2023); doi: 10.1063/5.0170627

Submitted: 3 August 2023 • Accepted: 6 September 2023 •

Published Online: 22 September 2023



View Online



Export Citation



CrossMark

Kalyani Patrikar<sup>a)</sup> and Anirban Mondal<sup>a)</sup>

## AFFILIATIONS

Department of Chemistry, Indian Institute of Technology Gandhinagar, Gujarat 382355, India

<sup>a)</sup>Authors to whom correspondence should be addressed: [kalyani.p@iitgn.ac.in](mailto:kalyani.p@iitgn.ac.in) and [amondal@iitgn.ac.in](mailto:amondal@iitgn.ac.in)

## ABSTRACT

Interlayers at electrode interfaces have been shown to reduce contact resistance in organic devices. However, there still needs to be more clarity regarding the role of microscopic properties of interlayer functionalized interfaces on device behavior. Here, we show that the impact of functionalized electrodes on device characteristics can be predicted by a few critical computationally derived parameters representing the interface charge distribution and orbital interactions. The significant influences of interfacial orbital interactions and charge distribution over device and interface properties are exhibited. Accordingly, a function is developed based on these parameters that capture their effect on the interface resistance. A strong correlation is observed, such that enhanced orbital interactions and reduced charge separation at the interface correspond to low resistance regardless of the individual molecules utilized as the interlayer. The charge distribution and orbital interactions vary with the molecular structure of the interlayer, allowing the tuning of device characteristics. Hence, the proposed function serves as a guideline for molecular design and selection for interlayers in organic devices.

Published under an exclusive license by AIP Publishing. <https://doi.org/10.1063/5.0170627>

Devices based on organic semiconductors (OSCs) have enabled several novel applications, such as flexible displays or wearable sensors.<sup>1,2</sup> Several *n*-type OSCs, such as Polyera ActivInk (N1400) or P(NDI2OD-T2) (N2200), have enabled high performance electron-transporting organic devices.<sup>3,4</sup> However, the device current remains limited due to the resistance at the hetero-interface of injecting electrodes and OSC, known as contact resistance ( $R_C$ ).<sup>5,6</sup>  $R_C$  acts in series with the resistance of the OSC layer and hence increases the total resistance of the device.  $R_C$  is reported to originate due to phenomena such as pillow effects, defect generation, and the induction of gap states, which accompany the energy level alignment process during interface formation.<sup>7</sup> These lead to the formation of an interface dipole that hinders electron injection from the electrode to the OSC.<sup>8</sup> As a remedy, interlayers are inserted at the interface of OSC and electrode, such as organic dopants or a self-assembled monolayer (SAM), in devices including organic field effect transistors (OFETs), organic photovoltaics (OPVs) or organic light-emitting diodes (OLEDs).<sup>9–11</sup> Organic interlayers have been demonstrated to effectively reduce the injection barrier and form ohmic contact where the interlayer helps to decouple the OSC and electrode

electrostatically.<sup>12</sup> It was shown that the presence of an interlayer diminishes the effect of the attractive image potential at the interface and eliminates the broadening of the density of states present at the OSC-electrode interface while restoring Fermi-level alignment. Polar interlayers such as SAM of polar organic molecules have been revealed to reduce the energy difference between the work function of the electrode ( $\phi$ ) and electron affinity (EA) of the OSC.<sup>13</sup> This reduces the energy barrier to electron injection from the electrode to the OSC and consequently reduces the contact resistance.<sup>14,15</sup> While studies have shown the effects of interlayers on energy level alignment and device properties, the role of interactions among the components of the contact interface has generally not been incorporated. Interestingly, it has been observed that the dipole moment of SAM does not directly determine the contact resistance of the device.<sup>16–18</sup> On the other hand, it has been established recently that orbital interactions at the electrode-OSC interface have a marked effect on the contact resistance and device characteristics, the contribution of which has generally not been considered significant.<sup>19</sup> Orbital interaction at the interface affects the charge transfer rate,<sup>20,21</sup> possibly creating gap states and altering energy level alignment.

In the past, first principle-driven molecular models have been developed to describe the effects of factors such as polarity on shifting the work function of electrodes, interactions between inorganic and organic components at the interface,<sup>22,23</sup> and length and orientation of interlayer molecules on resistance.<sup>24,25</sup> However, to the best of our knowledge, the ambiguity regarding the relative role of polarity and orbital interactions in reducing  $R_C$  remains unresolved, and no computational models are predicting their combined effect on  $R_C$ .

This study aims to develop a model to predict the effect of interlayer functionalized electrodes (IFEs) on organic devices' interface properties and contact resistance. Previous models based on first principles computations of SAM as an interlayer in organic devices have attempted to study their characteristics by simulating a layer of molecules attached to the electrode slab.<sup>26</sup> We show that the simulation of molecular parameters includes sufficient information to evaluate the efficiency of an interlayer in reducing  $R_C$ , thereby lessening the overall computational cost. We consider injection based on a hopping transport mechanism between the organic IFE and OSC. We seek to quantify the physical phenomenon associated with electron transfer at the interface. For this, parameters representing interface polarity and orbital interactions were defined, and their effect on interface and device properties was analyzed. We show that the charge distribution at the interface and the charge transfer integral of orbitals significantly influence interface and device behavior. Parameters were computed within a first principle framework, and the obtained results were validated against experimentally measured contact resistances of organic transistors and work functions of electrodes functionalized with SAM interlayers. Subsequently, a function was derived that could predict the effect of IFE on device characteristics and interface properties based on parameters computed for the particular interface, i.e., charge distribution and charge transfer integral. Experimental studies performed by Boudinet *et al.* on a variety of IFEs in the form of self-assembled monolayers deposited on Au electrodes in devices of *n*-type semiconductors were used to validate the model.<sup>27</sup> In their study, various device parameters are compared for SAM-functionalized electrodes comprising molecules that are aliphatic, aromatic, and with different substituent groups (see Fig. 1).<sup>27</sup> Contact resistance ( $R_C$ ) was measured by the transmission line method (TLM), which isolates the electrical resistance at the contact interface from bulk OSC.<sup>28</sup> Therefore, the values of  $R_C$  are the resistance to charge injection at the interface. The correlation of the function with these device measurements is demonstrated, asserting the combined effect of polarity and orbital interaction in determining contact resistance and a methodology for rapid evaluation of the efficiency of interlayer-modified contacts.

Density functional theory (DFT) based first principle computations were performed for the interface of IFE containing varying SAM interlayers and OSC. A slice of the contact interface comprising IFE and semiconductor was simulated. The IFE comprised an Au layer bonded to aliphatic or aromatic thiol molecules (Fig. 1). The position of the N1400 molecule (Fig. 1) next to IFE was optimized according to distance and angular criteria. The stack was set up with only a single molecule each from the SAM and OSC layers. Simulating such a stack aims to study the intermolecular interactions at the interface from first principles and understand their effect on device behavior. Parameters computed from this stack are valid for

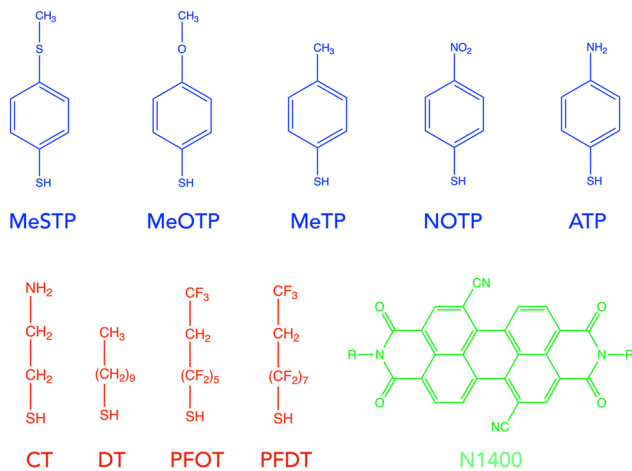


**FIG. 1.** Schematic of aromatic and aliphatic molecules forming self-assembled monolayers on gold (Au) contacts to form IFE, labeled according to the functional groups, along with the schematic of OSC N1400 constituting the OFET channel.

any position along the interface. Further, this approach minimizes computational costs and allows rapid screening of candidate SAM molecules.

We observe that the characteristics of interface orbitals vary for different interface stacks. Figure 2 shows the lowest unoccupied molecular orbitals (LUMO) generated via DFT calculations for the stacks with MeTP and PFDT interlayer SAM. It is apparent that the LUMO is highly delocalized over the MeTP-stack compared to the PFDT-stack. As the LUMO participates directly in the electron

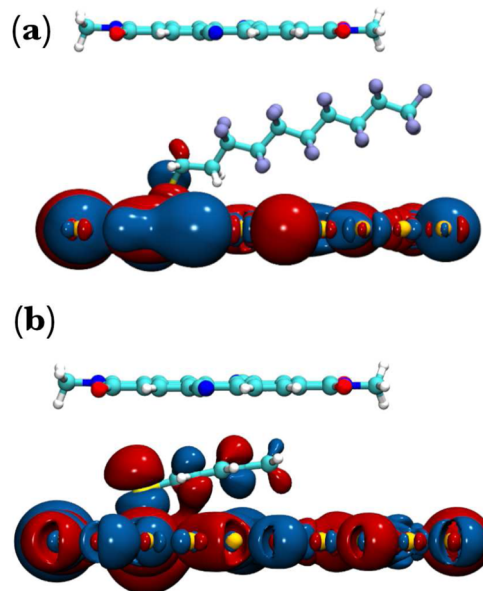


**FIG. 2.** LUMO generated via DFT simulations of interface stacks for IFE with (a) PFDT and (b) MeTP, displaying the marked difference in orbital delocalization for interfaces with different IFE, which correlates with the difference in  $R_C$ .

transfer across the interface, the extent of its delocalization indicates enhanced electron transfer from Au-MeTP to N1400 as compared to Au-PFDT to N1400. Accordingly, MeTP-stack and PFDT-stack correspond to the lowest and highest values of  $R_C$ , respectively, measured for N1400 transistors as given in Ref. 27.

During device operation, an electron hops from the IFE and gets localized over the LUMO of N1400. The correlation between frontier orbital interactions at the contact interface and the resulting contact resistance can be quantified based on the charge transfer rate between IFE and OSC.<sup>29</sup> As the electron transferred from IFE is localized on OSC, the rate of electron transfer can be estimated by the Marcus equation as given in Eq. (1). The Marcus equation can be considered a reasonable estimate of electron transfer to organic molecules, as the rigid nature of the components of the interface allows the nonadiabatic effects and vibronic coupling to be neglected.<sup>30</sup> The rate of electron hopping ( $k_{ij}$ ) between electronic sites  $i$  and  $j$  is given by Marcus equation as per Eq. (1),<sup>31</sup>

$$k_{ij} = \frac{J_{ij}^2}{\hbar} \sqrt{\frac{\pi}{\lambda kT}} \exp\left(\frac{-\lambda}{4kT}\right). \quad (1)$$

Here,  $\lambda$  is the reorganization energy, a measure of the physical rearrangement undergone by the system during electron transfer. IFE is a rigid system, while N1400 is expected to undergo rearrangement as it acquires the transferred electron. Hence, the properties of N1400 dominate  $\lambda$ , and here, they are assumed to be constant for all stacks.  $J_{ij}$  is the charge transfer integral between states  $i$  and  $j$ , thus measuring the feasibility of charge transfer between the site orbitals.  $J_{ij}$  was calculated for all stacks as per Eq. (2),<sup>32</sup>

$$J = \int \psi_i \mathcal{H} \psi_j dr^3. \quad (2)$$

Here,  $\psi_i$  and  $\psi_j$  are the LUMO of IFE and OSC, respectively. The value of  $J$  (replacing  $J_{ij}$  for simplicity in the future discussion) for the MeTP-stack is  $1.21 \times 10^{-2}$  eV, while  $J$  is  $2.40 \times 10^{-5}$  eV for the PFDT-stack. The values of  $J$  for all stacks are summarized in Table S1. Figure 3(a) shows the correlation between  $J$  for all IFE-OSC systems and the measured  $R_C$  for N1400 transistors in Ref. 27. An increase in the  $J$  of the stack evidently reduces the device's  $R_C$ . However, some exception interfaces with higher values of  $J$  do not lead to lower  $R_C$ . This anomaly is because, while  $J$  is related to the rate of electron transfer at the interface, it contains no information on the number of electrons or charges transferred.

The interface's polarity is understood to influence  $R_C$  substantially.<sup>6</sup> The presence of SAM modulates the interface dipole, depending on the functional groups attached to the SAM molecule and the interactions between IFE and OSC at the interface. Attachment of SAM leads to a shift in  $\varphi$  of the electrode and consequently affects the energy level alignment during interface formation, which determines the interface dipole.<sup>16</sup> The computation of interface dipoles by first principle methods is challenging as it requires separating IFE and OSC components within the stack. However, partial charges on IFE and OSC can be obtained from DFT-based computations, representing the charge separation between these components and, consequently, the dipole at the interface. The partial charge on OSC ( $Q$ ) for all stacks was computed via DFT. The magnitude of  $Q$  depends on  $\varphi$  of the IFE. Figure 3(b) shows the correlation between measured  $\varphi$  for all IFEs as given in Ref. 27 and  $Q$  obtained

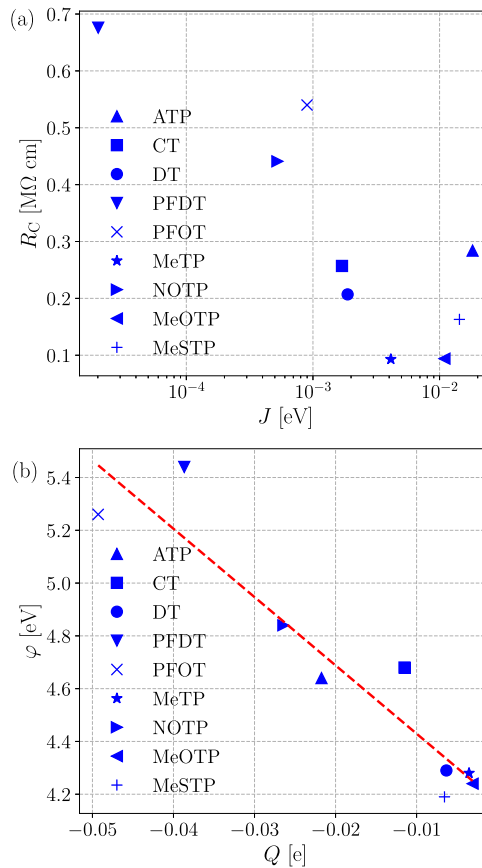


**FIG. 3.** (a) Correlation between measured contact resistance  $R_C$ <sup>27</sup> and computed charge transfer integral  $J$ . (b) Work functions ( $\varphi$ ) of IFEs<sup>27</sup> correlated against the net charge accumulation,  $Q$ .

by DFT computations for the corresponding stack. As evident from Fig. 3(b),  $Q$  estimates the effect of  $\varphi$  of the electrode on equilibrium conditions at the IFE-OSC interface.  $\varphi$  of IFE with MeTP is  $-4.18$  eV, while  $\varphi$  is  $-5.44$  eV for IFE with PFDT. Corresponding to this,  $Q$  for MeTP-stack is  $3.52 \times 10^{-3}$  e, while it is  $3.86 \times 10^{-2}$  e for PFDT-stack. The values of  $Q$  for all stacks are summarized in Table S1. Essentially, an IFE with a low value of  $\varphi$  favors electron injection and corresponds to a low magnitude of charge separation at the interface. The low magnitude of  $Q$ , and hence a low interface dipole, reduces hindrance to an injecting electron.

It is apparent that both the parameters  $J$  and  $Q$  influence the resistance at the IFE-OSC interface, as these determine the feasibility of charge transfer and measure the effect of electrode work function. However, neither of them is sufficient to predict the  $R_C$  of the organic device independently. Therefore, a model capable of predicting the  $R_C$  of devices with IFE must combine the effects of both  $Q$  and  $J$ , encompassing the effects of orbital interactions as well as the work function of IFE. While forming the function,  $J$  is represented in the form of a log to obtain values numerically comparable to those of  $Q$  and magnify the differences in their values among all IFE-OSC combinations. A high value of  $J$  leads to low  $R_C$ ; as the numerical

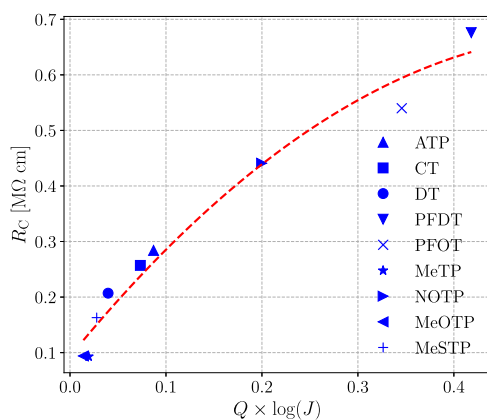


**FIG. 4.** Function combining computed quantities  $Q$  and  $J$  predicting the measured  $R_C$  of the device.<sup>27</sup> Fit is displayed as a guide.

value of  $J$  is always less than one, a low value of  $\log(J)$  leads to low  $R_C$ . Similarly, a minimum value of  $Q$  leads to a low  $R_C$ . Hence, a product of these two quantities leads to a function ( $f$ ) as given in Eq. (3) that needs to be minimized for a functionalized interface to obtain a low  $R_C$  in the device,

$$f = Q \times \log(J). \quad (3)$$

Figure 4 shows the plot of  $f$  with the devices' experimentally measured  $R_C$ .<sup>27</sup> As can be seen, a high magnitude of  $f$  corresponds to a high  $R_C$ , with a quadratic fit displayed as a guide. The closeness of the fit indicates that  $f$  can be employed to assess a particular stack for resulting device behavior.

The significance of  $f$  can be explained by considering devices with MeSTP and MeTP stacks. For the interface of MeSTP-Au and OSC, the value of  $J$  ( $2.60 \times 10^{-2}$  eV) is higher than the interface of MeTP-Au and OSC ( $7.08 \times 10^{-3}$  eV), indicating better electron injection in the device with MeSTP. Contrasting this, the value of  $Q$  is higher for the MeSTP-stack with  $6.56 \times 10^{-3} e$  compared to the MeTP-stack with  $3.52 \times 10^{-3} e$ . As a result, the magnitude of  $f$  and, accordingly, the value of  $R_C$  become larger in the MeSTP-stack than the MeTP. This trade-off between  $J$  and  $Q$  is evident from Fig. 4, which depicts the combined effects of  $Q$  and  $\log(J)$  that predict a lower  $R_C$  for devices with a MeTP-stack than that for a MeSTP stack. Analogously, the  $Q$  of the PFDT-stack ( $3.86 \times 10^{-2} e$ ) is lower than that of the PFOT-stack ( $4.92 \times 10^{-2} e$ ), indicating the feasibility of electron transfer is greater at the interface with the PFDT stack. However,  $J$  for the PFOT-stack ( $1.41 \times 10^{-3}$  eV) is significantly higher than that for PFDT, which is  $2.40 \times 10^{-5}$ . Overall, this leads to the value of  $f$  for the PFOT-stack having a lower magnitude than that of PFDT. Correspondingly, the  $R_C$  for the device with the PFOT-stack is lower than the PFDT-stack. Therefore, we demonstrate that  $f$  provides an effective combination of  $Q$  and  $J$ , which correlates strongly to the device  $R_C$ . The high correlation demonstrates that representing the orbital interactions and the charge separation at the interface comprehensively captures the role of an interlayer in modifying interface conditions at device contacts.

Furthermore, the role of parameters  $Q$  and  $J$ , particularly the functional form of  $f$ , is explored for their influence on the interface

conditions in the device. The process of energy level alignment during interface formation is accompanied by charge transfer across the interface. According to Poisson's equation, the equilibrium charge carrier density at interface  $n(0)$  can be estimated based on the interface energy barrier  $\phi_0$ .  $\phi_0$  has been reported to depend on  $\varphi$  of IFE and electron affinity (EA) for OSC.<sup>12</sup> Based on electronic structure calculations, the EA of N1400 was found to be 3.67 eV. The form Poisson's equation takes for the conditions at the interface at equilibrium is given in the following equation:<sup>33</sup>

$$\frac{\partial^2 \phi(x)}{\partial x^2} = \frac{qn(x)}{\epsilon\epsilon_0}, \quad (4)$$

$$\lim_{x \rightarrow \infty} \frac{\partial \phi(x)}{\partial x} = 0, \quad n(0) = N \exp \frac{-q\phi(0)}{kT}.$$

Here,  $\phi(x)$  is the potential and  $n(x)$  is the charge carrier density at position  $x$  away from the interface in the semiconductor. Accordingly,  $\phi(0)$  at  $x = 0$  at the interface refers to the potential barrier to charge injection. The potential barrier can be evaluated as  $(\varphi - EA)$  with an additional pinning barrier, which has been reported to be estimated at 0.3 eV, adding to the injection barrier.<sup>34</sup> Applying this approximation,  $\phi(0)$  was calculated for each IFE-OSC interface based on the measured  $\varphi$  for IFE reported in Ref. 27. The dielectric constant was assumed to be 3.5 for the OSC. Subsequently, Eq. (4) yielded  $n(0)$  for these interfaces. Figure 5 displays  $n(0)$  for the IFE-OSC interface plotted against  $f$ .

As seen from Fig. 5, a clear trend is visible, with the magnitude of charge carrier density being nearly linear with the value of  $f$ . A low value of  $f$  corresponds to an interface with a high  $n(0)$ , and hence an interface capable of transferring a larger magnitude of charge, and therefore an interface with a lower  $R_C$ . This asserts that the contribution of interlayer molecules in determining the interface conditions can be predicted based on the combination of  $Q$  and  $J$  as contained in  $f$ .  $n(0)$  is related to  $R_C$  such that an interface having a lower resistance is capable of transferring a larger magnitude of charge. On the other hand, the parameters  $J$  and  $Q$  represent microscopic elements of the interface that determine its resistance and, therefore, correlate with  $n(0)$ . As a result,  $f$ , which combines  $J$  and  $Q$ , can predict not just  $R_C$  but  $n(0)$  as well by including the

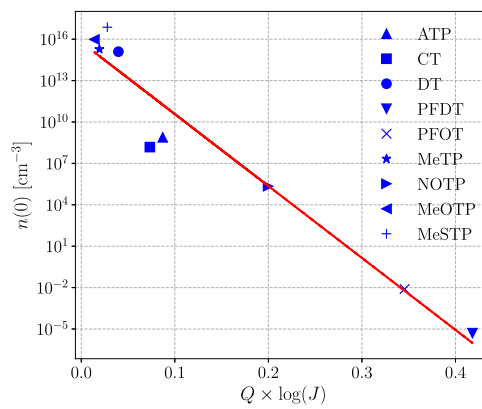


**FIG. 5.** Dependence of the charge carrier density on the model function  $f$ . The dotted line represents a guide to the eyes.

parameters most relevant to charge injection at the interface. Similarly, we note that the interlayer's effect in determining the device's electron mobility can also be predicted based on the value of  $f$ , as exhibited in Fig. S1 of SI. These observations assert the role of  $Q$  and  $J$ , particularly the form taken by  $f$ , in predicting the effect of an IFE on device behavior.

To summarize, we show that a combination of interface charge distribution and orbital interactions at the interface determine the  $R_C$  of devices with IFE. These effects are captured by computationally derived parameters  $Q$  and  $J$ . We show that parameters derived from computations performed on a stack comprising a molecule each from the OSC and SAM interlayers correlate strongly with device characteristics, as validated with measured  $\varphi$  on IFE and device  $R_C$ .  $Q$  represents the influence of  $\varphi$  of IFE and interface polarity. At the same time,  $J$  quantifies interfacial orbital interactions, which affect the feasibility of charge transfer from the IFE to the semiconductor. These are combined into a function  $f$  to obtain a combination of the parameters that predict the effect of interlayer at the interface and, consequently, the device's performance.  $f$  correlates strongly with the experimentally measured values of  $R_C$ ; it is found that a minimum of  $R_C$  is achieved for interfaces leading to lower values of  $f$ . We find that while  $f$  is obtained by computations of only a minimalistic stack of the device containing a part of the surface of the metal and a single molecule, each of interlayer and OSC, respectively, it is capable of predicting device behavior. Therefore, the approach presented significantly reduces the tedium of experimental testing for selecting an interlayer for a given organic device and acts as a guideline for efficient molecular design. We effectively establish a strategy to predict the performance of an IFE in organic devices solely based on the computation of the electrode surface, an interlayer molecule, and a semiconductor molecule.  $f$  can be treated as a universal guideline for selecting an IFE-semiconductor system to obtain the required device characteristics.

## SUPPLEMENTARY MATERIAL

The supplementary material contains details of computational methods, a table of computed values, and a figure displaying the relation between the function described in Eq. (3) and device mobility.

## ACKNOWLEDGMENTS

The authors gratefully acknowledge the Indian Institute of Technology, Gandhinagar, India, for providing research facilities and financial support. A.M. acknowledges the SERB (Grant No. SRG/2022/001532) project for funding. K.P. and A.M. acknowledge PARAM Ananta for computational resources.

## AUTHOR DECLARATIONS

### Conflict of Interest

The authors have no conflicts to disclose.

### Author Contributions

**Kalyani Patrikar:** Data curation (equal); Formal analysis (equal); Investigation (equal); Methodology (equal); Validation (equal);

Writing – original draft (equal); Writing – review & editing (equal). **Anirban Mondal:** Conceptualization (equal); Data curation (equal); Formal analysis (equal); Funding acquisition (equal); Investigation (equal); Methodology (equal); Project administration (equal); Resources (equal); Supervision (equal); Validation (equal); Writing – original draft (equal); Writing – review & editing (equal).

## DATA AVAILABILITY

The data that support the findings of this study are available from the corresponding authors upon reasonable request.

## REFERENCES

- <sup>1</sup>Y. Yin, M. U. Ali, W. Xie, H. Yang, and H. Meng, "Evolution of white organic light-emitting devices: From academic research to lighting and display applications," *Mater. Chem. Front.* **3**, 970–1031 (2019).
- <sup>2</sup>Y. H. Lee, O. Y. Kweon, H. Kim, J. H. Yoo, S. G. Han, and J. H. Oh, "Recent advances in organic sensors for health self-monitoring systems," *J. Mater. Chem. C* **6**, 8569–8612 (2018).
- <sup>3</sup>G. Casula, S. Lai, L. Matino, F. Santoro, A. Bonfiglio, and P. Cosseddu, "Printed, low-voltage, all-organic transistors and complementary circuits on paper substrate," *Adv. Electron. Mater.* **6**, 1901027 (2020).
- <sup>4</sup>T. Steckmann, I. Angunawela, S. Kashani, Y. Zhu, M. M. Nahid, H. Ade, and A. Gadisa, "Ultrathin P(NDI2OD-T2) films with high electron mobility in both bottom-gate and top-gate transistors," *Adv. Electron. Mater.* **8**, 2101324 (2022).
- <sup>5</sup>M. Waldrip, O. D. Jurchescu, D. J. Gundlach, and E. G. Bittle, "Contact resistance in organic field-effect transistors: Conquering the barrier," *Adv. Funct. Mater.* **30**, 1904576 (2020).
- <sup>6</sup>Y. Xu, H. Sun, and Y.-Y. Noh, "Schottky barrier in organic transistors," *IEEE Trans. Electron Devices* **64**, 1932–1943 (2017).
- <sup>7</sup>D. Natali and M. Cairoli, "Charge injection in solution-processed organic field-effect transistors: Physics, models and characterization methods," *Adv. Mater.* **24**, 1357–1387 (2012).
- <sup>8</sup>F. Amy, C. Chan, and A. Kahn, "Polarization at the gold/pentacene interface," *Org. Electron.* **6**, 85–91 (2005).
- <sup>9</sup>J. Frisch, H. Glowatzki, S. Janietz, and N. Koch, "Solution-based metal electrode modification for improved charge injection in polymer field-effect transistors," *Org. Electron.* **10**, 1459–1465 (2009).
- <sup>10</sup>F. Huang, H. Liu, X. Li, and S. Wang, "Highly efficient hole injection/transport layer-free OLEDs based on self-assembled monolayer modified ITO by solution-process," *Nano Energy* **78**, 105399 (2020).
- <sup>11</sup>Y. Lin, Y. Zhang, J. Zhang, M. Marcinkas, T. Malinauskas, A. Magomedov, M. I. Nugraha, D. Kaltsas, D. R. Naphade, G. T. Harrison *et al.*, "18.9% efficient organic solar cells based on n-doped bulk-heterojunction and halogen-substituted self-assembled monolayers as hole extracting interlayers," *Adv. Energy Mater.* **12**, 2202503 (2022).
- <sup>12</sup>N. B. Kotadiya, H. Lu, A. Mondal, Y. Ie, D. Andrienko, P. W. Blom, and G.-J. A. Wetzelar, "Universal strategy for Ohmic hole injection into organic semiconductors with high ionization energies," *Nat. Mater.* **17**, 329–334 (2018).
- <sup>13</sup>I. H. Campbell, S. Rubin, T. A. Zawodzinski, J. D. Kress, R. L. Martin, D. Smith, N. N. Barashkov, and J. P. Ferraris, "Controlling Schottky energy barriers in organic electronic devices using self-assembled monolayers," *Phys. Rev. B* **54**, R14321 (1996).
- <sup>14</sup>L. Han, Y. Huang, W. Tang, S. Chen, J. Zhao, and X. Guo, "Reducing contact resistance in bottom contact organic field effect transistors for integrated electronics," *J. Phys. D: Appl. Phys.* **53**, 014002 (2019).
- <sup>15</sup>A. Petritz, M. Krammer, E. Sauter, M. Gärtner, G. Naschimbeni, B. Schröde, A. Fian, H. Gold, A. Cojocaru, E. Karner-Petritz *et al.*, "Embedded dipole self-assembled monolayers for contact resistance tuning in p-type and n-type organic thin film transistors and flexible electronic circuits," *Adv. Funct. Mater.* **28**, 1804462 (2018).
- <sup>16</sup>C. Liu, Y. Xu, and Y.-Y. Noh, "Contact engineering in organic field-effect transistors," *Mater. Today* **18**, 79–96 (2015).

- <sup>17</sup>M. M. Thuo, W. F. Reus, C. A. Nijhuis, J. R. Barber, C. Kim, M. D. Schulz, and G. M. Whitesides, "Odd-even effects in charge transport across self-assembled monolayers," *J. Am. Chem. Soc.* **133**, 2962–2975 (2011).
- <sup>18</sup>P. Marmont, N. Battaglini, P. Lang, G. Horowitz, J. Hwang, A. Kahn, C. Amato, and P. Calas, "Improving charge injection in organic thin-film transistors with thiol-based self-assembled monolayers," *Org. Electron.* **9**, 419–424 (2008).
- <sup>19</sup>K. Patrikar, U. Bothra, V. R. Rao, and D. Kabra, "Charge carrier doping as mechanism of self-assembled monolayers functionalized electrodes in organic field effect transistors," *Adv. Mater. Interfaces* **9**, 2101377 (2022).
- <sup>20</sup>H. Vázquez, W. Gao, F. Flores, and A. Kahn, "Energy level alignment at organic heterojunctions: Role of the charge neutrality level," *Phys. Rev. B* **71**, 041306 (2005).
- <sup>21</sup>H. Ishii, K. Sugiyama, E. Ito, and K. Seki, "Energy level alignment and interfacial electronic structures at organic/metal and organic/organic interfaces," *Adv. Mater.* **11**, 605–625 (1999).
- <sup>22</sup>G. Heimel, L. Romaner, E. Zoyer, and J.-L. Brédas, "Toward control of the metal-organic interfacial electronic structure in molecular electronics: A first-principles study on self-assembled monolayers of  $\pi$ -conjugated molecules on noble metals," *Nano Lett.* **7**, 932–940 (2007).
- <sup>23</sup>G. Heimel, L. Romaner, E. Zoyer, and J.-L. Bredas, "The interface energetics of self-assembled monolayers on metals," *Acc. Chem. Res.* **41**, 721–729 (2008).
- <sup>24</sup>G. Heimel, L. Romaner, J.-L. Brédas, and E. Zoyer, "Odd- even effects in self-assembled monolayers of  $\omega$ -(biphenyl-4-yl) alkanethiols: A first-principles study," *Langmuir* **24**, 474–482 (2008).
- <sup>25</sup>I. Katsouras, V. Geskin, A. J. Kronemeijer, P. W. Blom, and D. M. de Leeuw, "Binary self-assembled monolayers: Apparent exponential dependence of resistance on average molecular length," *Org. Electron.* **12**, 857–864 (2011).
- <sup>26</sup>G. Heimel, L. Romaner, J.-L. Brédas, and E. Zoyer, "Organic/metal interfaces in self-assembled monolayers of conjugated thiols: A first-principles benchmark study," *Surf. Sci.* **600**, 4548–4562 (2006).
- <sup>27</sup>D. Boudinet, M. Benwadih, Y. Qi, S. Altazin, J.-M. Verilhac, M. Kroger, C. Serbutovitz, R. Gwoziecki, R. Coppard, G. Le Blevennec *et al.*, "Modification of gold source and drain electrodes by self-assembled monolayer in staggered n- and p-channel organic thin film transistors," *Org. Electron.* **11**, 227–237 (2010).
- <sup>28</sup>R. Rödel, F. Letzkus, T. Zaki, J. Burghartz, U. Kraft, U. Zschieschang, K. Kern, and H. Klauk, "Contact properties of high-mobility, air-stable, low-voltage organic n-channel thin-film transistors based on a naphthalene tetracarboxylic diimide," *Appl. Phys. Lett.* **102**, 233303 (2013).
- <sup>29</sup>A. Köhler and H. Bässler, *Electronic Processes in Organic Semiconductors: An Introduction* (John Wiley & Sons, 2015).
- <sup>30</sup>R. P. Fornari, J. Aragó, and A. Troisi, "A very general rate expression for charge hopping in semiconducting polymers," *J. Chem. Phys.* **142**, 184105 (2015).
- <sup>31</sup>A. Troisi, A. Nitzan, and M. A. Ratner, "A rate constant expression for charge transfer through fluctuating bridges," *J. Chem. Phys.* **119**, 5782–5788 (2003).
- <sup>32</sup>E. F. Valeev, V. Coropceanu, D. A. da Silva Filho, S. Salman, and J.-L. Brédas, "Effect of electronic polarization on charge-transport parameters in molecular organic semiconductors," *J. Am. Chem. Soc.* **128**, 9882–9886 (2006).
- <sup>33</sup>I. Gutiérrez Lezama and A. Morpurgo, "Threshold voltage and space charge in organic transistors," *Phys. Rev. Lett.* **103**, 066803 (2009).
- <sup>34</sup>M. T. Greiner, M. G. Helander, W.-M. Tang, Z.-B. Wang, J. Qiu, and Z.-H. Lu, "Universal energy-level alignment of molecules on metal oxides," *Nat. Mater.* **11**, 76–81 (2012).